Manipulating Short-Lived Isotopes with Inhomogeneous RF-Fields

T. Li and H. A. Schuessler

Texas A&M University, College Station, Texas, USA

Abstract: Online isotopes separators (ISOL-systems) and projectile fragment separators provide a wide variety of radioactive ions with energies in the keV to the several MeV ranges. For high resolution radio frequency and optical spectroscopy the ions must be decelerated to low energies and possibly injected into an ion trap. With this goal in mind we have made simulations of ion orbits under the influence of strong focusing by inhomogeneous RF fields and decelerating DC fields. The operation of the segmented linear ion guide, the ion carpet, and the ion funnel are discussed. The optimum operating parameters of these devices are obtained using computer simulations with SIMION software.

INTRODUCTION

Strong focusing in an inhomogeneous RF-field is a well known feature where the time average of the alternating RF force on an ion is directed towards the region of the weaker field [1]. This property is widely employed for the focusing of ion beams, for selective transmission in mass filters [2], and for ion storage in RF- and combined ion-traps [3,4]. In particular, the manipulation, bunching, storage and injection of externally generated ions have depended on it. RF-ion guides have also been used in chemistry [5] and atomic physics [6]. Radio frequency quadrupole accelerators (RFQ) [7] have been employed in accelerator physics. Recently quadrupole ion guides [8] were adapted to the new radioactive beam facilities and are already in use at some of these and other facilities. Such ion guides also provide the radial confinement during buffer gas cooling of short-lived isotopes being produced on-line at nuclear facilities. In this paper we present construction principles and simulations of ion orbits for three novel focusing devices which are all based on inhomogeneous RF-fields. These devices are the segmented ion-guide, the ion-carpet and the ion-funnel.

ION FOCUSING DEVICES

The purpose of ion focusing devices is to collimate, to confine during cooling by viscous buffer gas collisions, and eventually to trap short-lived isotope ions produced on-line. A high collection efficiency is a major design requirement, since the new radioactive beam facilities produce only minute amounts of short-lived signal ions far off stability. In general, the strong primary beam must also be suppressed. The latter condition is effected by either a fragment separator for high energy reaction products (about 100 Mev/u) or by an on-line isotope separator for lower energy beams (about 50 keV). Once the ions are decelerated and trapped, the vacuum is in the UHV-region between 10^{-7} and 10^{-11} torr, to allow the storage of the short-lived isotopes for their nuclear half-life.

The segmented RF-ion guide: Figure 1 shows our test setup for an RF-ion guide consisting of 10 segments. Each segment is made up of four circular electrodes (diameter Φ=6mm, seperation between opposing electrodes d=12mm, length l=15mm). The RF-voltage is applied between the horizontal and vertical pairs of the various electrodes. For simulating the effect of buffer gas cooling, a damping factor of γ=0.07 corresponding to about 10^{-2} torr of helium was used. The damping factor of the SIMION software [9] can be related to the mobility parameter of ions in gases and gives time averaged ion trajectories. In the example we assumed an incident ion beam energy of 5 keV. The results can readily be scaled to higher energies if needed. In the present case the first ion guide segment is at 4.980 keV, and a properly designed einzel lens couples the ion beam into the setup. The optimum design of the parabolic entrance section is also shown. The operation of the segmented ion guide in various modes is depicted in Fig.2. The whole ion guide is thereby at the high voltage, and there is also a small DC gradient along the various segments of the device. A complete description of a working ion guide is given, for example, in reference [7].

The ion carpet: Figure 3 shows a picture of the ion carpet as used in reference [10]. It consists of many coaxial ring electrodes printed with gold plating on a plane circuit board. The large

CP680, *Application of Accelerators in Research and Industry: 17th Int'l. Conference,* edited by J. L. Duggan and I. L. Morgan

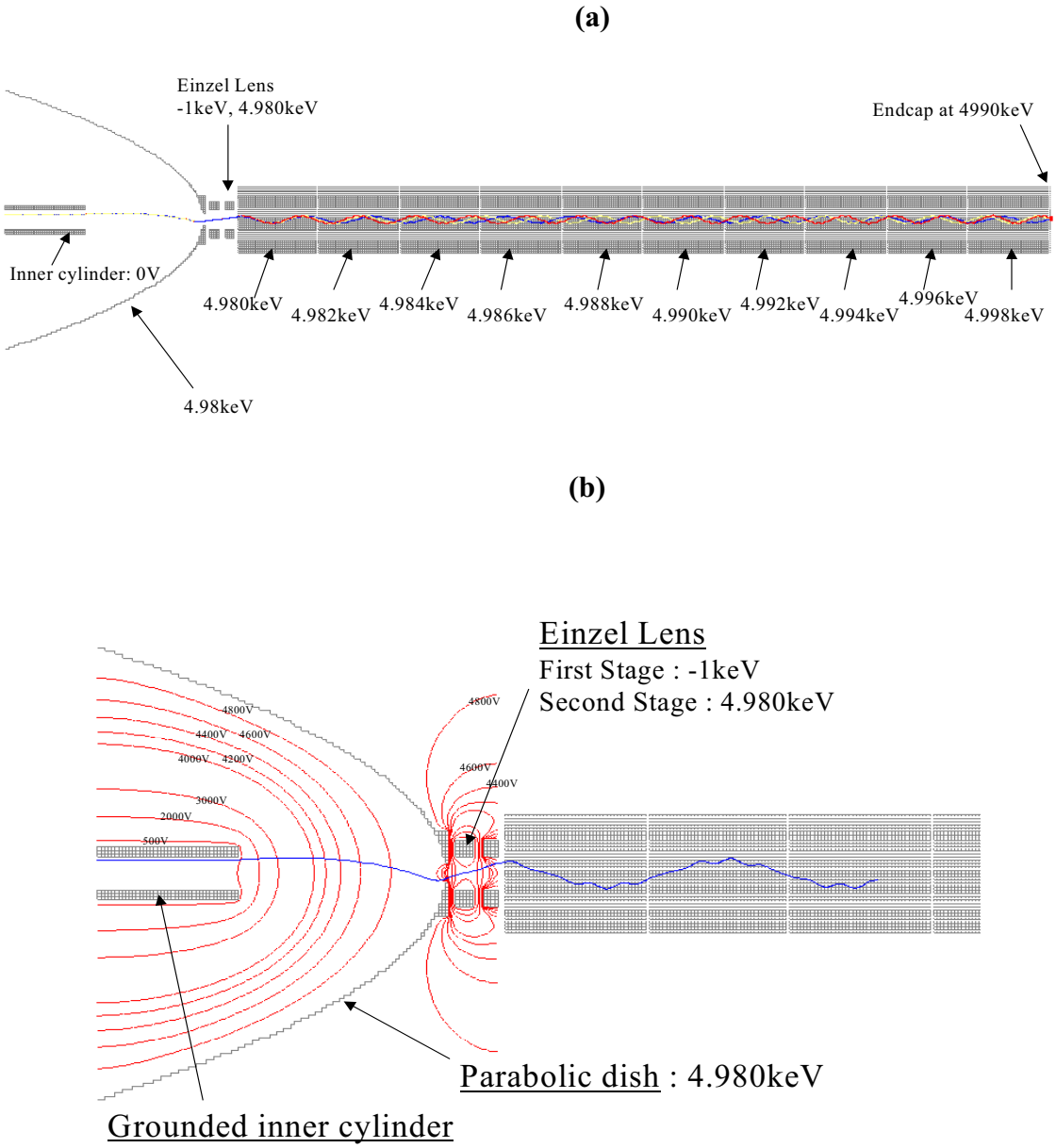

Figure 1 Diagram of the segmented ion guide (a) The DC – voltages are shown. The same phase RF-voltage is applied to opposite rods. (b) Potential distribution for optimum deceleration and injection into the guide.

opening in the center holds a second ring system behind it with a very small ring spacing and an exit hole of about 0.5 mm at the center.

In order to approximately simulate the operation of the device, we made a model consisting of a disc with 29 coaxial rings and a collection plate. The diameters of the rings vary from 1 mm to 30mm, the radial spatial period of the electrodes is 1mm. The diameter of the center hole is 1mm. A collection plate electrode is placed on axis 1mm behind the disk. SIMION software was again used to calculate the ion trajectories. The RF voltage is applied between adjacent rings, i.e. the phase of the voltage differs by 180° from one electrode to the other. In addition, a DC gradient is applied and is directed radially from the outer electrode to the center. The frequency and amplitude of the RF voltage and the DC gradient are variables in the program. Figure 4 shows typical ion projectiles. Ions are injected from the left to the right. A damping effect is added to simulate buffer gas

cooling. As can be seen, a typical trajectory consists of 4 sections: 1) The decelerating section where the high-energy ions go through the buffer gas and reduce their speed by collision with the buffer gas atoms. The speed of the ions is relatively high in this section, so the electric field in the device hardly changes the direction of the ions. This section therefore displays straight lines for the ions. In the approach section 2), the ions move with a constant low velocity, when the damping force balances the electric force. In this situation the trajectory is a smooth curve approaching the surface of the electrodes. Since the ions are still far above the electrode surface only very small oscillations can be observed there.

In the transport section 3) when the ions closely approach the surface, they are exposed to the strong inhomogeneous RF field between the electrodes, and are therefore repelled from the surface. In addition, they are also pushed by the centripetal component of the static electric field force. The overall effect is a trajectory parallel to the disc surface with strong oscillations moving toward the center. In the capture section 4) an ion reaches its destination, namely the center of the ion carpet, where the negatively biased collection plate captures them. In the simulation we used a single electrode. In a real device an ion guide and/or an ion trap would take the place of the captive plate.

To study the ion motion in the transport section in detail, the trajectories were also evaluated for different RF amplitude and frequency settings. With all other parameters kept constant, we can

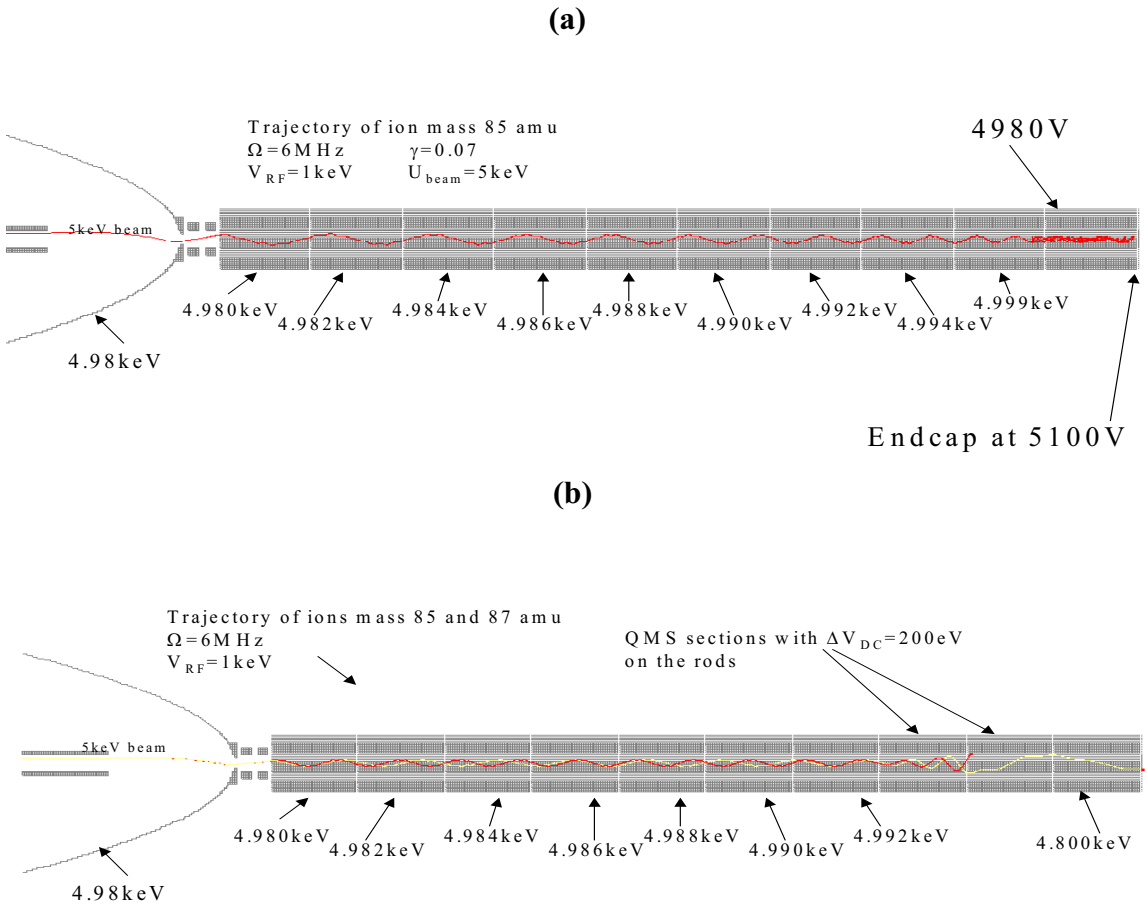

Figure 2 Operational modes of the ion guide. (a) The end section is an ion trap. (b) The end section passes the isotopes of interest and works as a mass separator.

clearly see that a higher RF voltage repels ions farther away from the surface. In this series of trajectories RF-voltages around 150V are optimum. With the same DC gradient applied, the speed of the ions remains similar. Therefore a lower frequency, i.e. a slower change in RF field, results in bigger oscillations in the ion trajectories, which decrease the stability of the transport section. A compromise should be made between the applied frequency and the trajectory stability. Experimentally, an efficiency of about 10^{-2} for guiding $^{8}Li^{+}$ions initially produced at about 100 MeV/u to the small exit hole in the center of the ion carpet was demonstrated in reference [10].

The ion funnel: In the ion funnel the arrangement consisting of a stack of ring shaped electrodes has a tapered inside envelope forming the funnel-like structure depicted in Fig.5. In our simulation the ion funnel consists of 30 parallel square shaped electrodes with circular inner openings. The first 10 electrodes have the same inner diameter. The diameter of the next 20 electrodes decreases linearly, and, in this way, the cone-shaped inner cavity is formed. The total length of the devices is 120 mm, the diameter of the cylindrical part is 90 mm. The electrodes are 6 mm apart in the cylinderical section, and 3 mm in the cone- like section. Ions

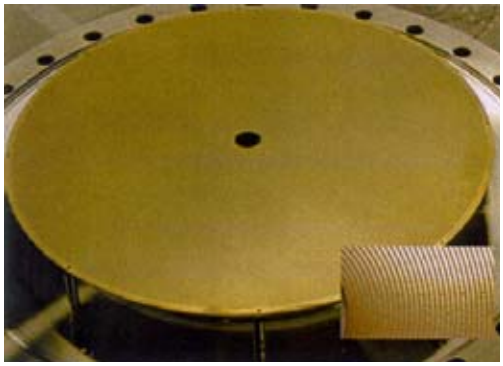

Figure 3 Photograph displaying the RF-electrode assembly on plane PCB with gold plated rings. A part of the electrode is enlarged in the bottom right (reprinted from [10] with permission from Elsevier).

were launched at the wide funnel entrance and collected at the exit behind the small hole on the other end. Also here the deceleration, approach, transport, and capture sections are seen. The micro motion shows up in the magnified trajectory in the transition from the approach section and in the entire transport section.

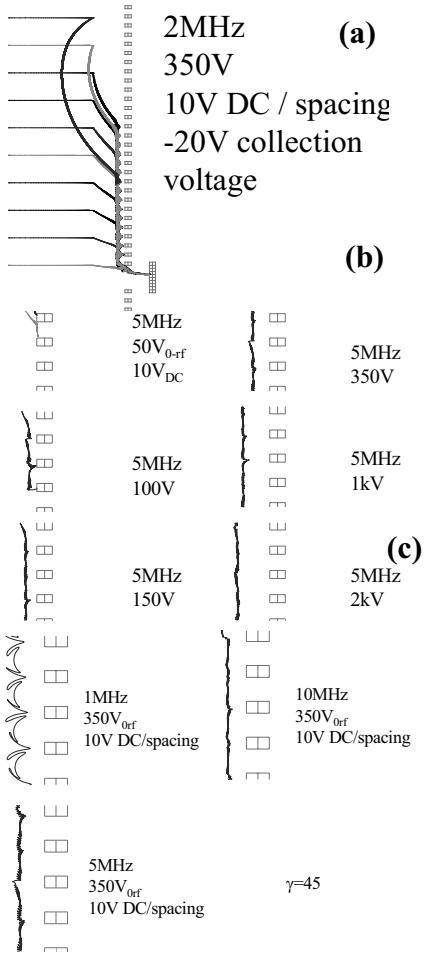

Figure 4 Typical ion trajectories. (a) The experimental parameters are : E= 70 keV, buffer gas damping factor γ =45. (b) Trajectories versus RF- amplitude. (c) Trajectory versus RF-frequency.

Monte Carlo simulation: This method was employed to find the optimum DC-RF combination for the operation of the ion funnel collector. A program was written to generate random DC-RF pairs, and then ions were launched with such randomly selected parameters.

The program records the numbers of ion orbits reaching the collection plate at the funnel exit with their corresponding conditions into a data file. The data were collected and, processed by Origin software, where the random data points (DC gradient as x axis, RF voltage as y axis, number of ions launched as z-axis) were converted into a grid matrix. By using a linear correlation method, we converted the data points to a 15-by-15-grid matrix. Figure 6 compiles the

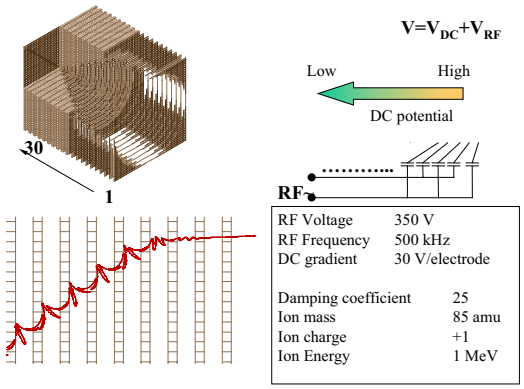

Figure 5 Ion Funnel (a) 3d plot of the ion funnel. (b) Cross section with operating voltages. (c) Ion trajectory

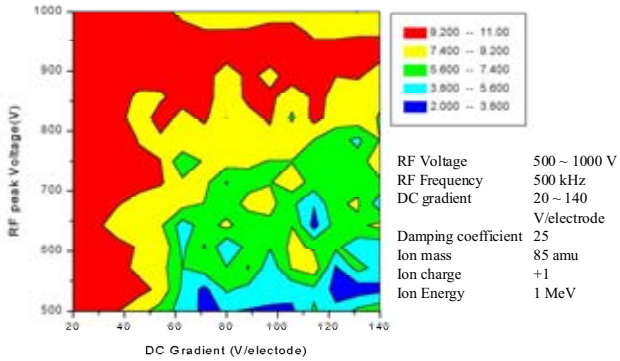

Figure 6 Contour plot for the operating parameters of the ion funnel

contour graph of the results. The higher the numerical value of the gray scale code, the higher the collection efficiency. It can be seen

that higher efficiencies are achieved with higher RF voltages and a lower DC gradient. This result is not surprising because the effect of the DC gradient is to push the ions through the cavity, while the RF voltage keeps them away from the surface. Thus, if we prefer low operating voltages without compromising on efficiency, we have optimum conditions at the values in the bottom left corner of the graph.

ACKNOWLEDGEMENT

This work is supported by the Robert A Welch Foundation under grant A 1546.

REFERENCES

1. H. G. Dehmelt, in Advances of Atomic and Molecular Physics, Vol 3, 53 (1967)
2. W. Paul and H. Steinwedel, Z. Naturforsch **89**, 448 (1953)
3. H. A. Schuessler, in Progress in Atomic Spectroscopy B, 999 (1979)
4. T. Nakamura, S. Ohtani, M. Wada, K. Okada, I. Katayama and H. A. Schuessler, J. Appl. Physics **89**. 2922 (2001)
5. E. Telog and D. Gerlich Chem. Phys. **4**, 417 (1974)
6. A. V. Tolmaduv, I. V. Chernuskevich, A. F. Dodonov, and K. G. Standing, Nucl. Instr. And Methods **B 124**, 112 (1997)
7. O. Kester, D. Hass, T. Sieber, M. Gloss, A. Kolbe, U. Koester, A. Schempp and U. Ratzingo, Nucl. Instr. and Methods **B 139**, 28 (1998)
8. H. Herfurth, J. Dilling, A. Kellerbauer, G. Bollen, S. Henry, H. J. Kluge, E. Lawour, D. Lunney, R. B. Moore, C. Scheidenberger, S. Schwarz, G. Sickler, J. Szerpd, Nucl. Instr. and Methods **A 33** (2000)
9. D. A. Dahl, in Simion Version 7.0 User Manual, published by Idaho National Engineering and Environmental laboratory (2000)
10. M. Wada,Y. Ishida, T. Nakamura, Y. Yamazaki, T. Kambara, H. Ohyama, Y. Kanai, T.M. Kojima, Y. Nakai, N. Ohshima, A. Yoshida, T. Kubo, Y. Matsuo, Y. Fukuyama, K. Okada, T. Sonoda, S. Ohtani, K. Noda, H. Kawakami, I. Katayama, Nucl. Instr. and Methods B (10 January 2003).
11. T. Kim et al, Analytical Chemistry **72**, 2247(2000).